A Shock-Wave Stress Gauge Utilizing the Capacitance Change of a Solid Dielectric Disc*

R. A. Graham and G. E. Ingram

Sandia Laboratory, Albuquerque

For publication in the Proceedings IUTAM Colloquium on the Behavior of Dense Media Under High Dynamic Pressures to be held in Paris, France, Sept. 11-15, 1967.

*This work was supported by the U. S. Atomic Energy Commission.

DISCLAIMER

A Shock-Wave Stress Gauge Utilizing the

Capacitance Change of a Solid Dielectric Disc

I. INTRODUCTION

The stress-time profiles which result when solids are subjected to shock-wave loading exhibit considerable detail when observed with fast time-resolution devices such as Sandia quartz gauges[1,2] air dielectric capacitors,[3-6] and laser interferometer devices.[7-9] Wave profiles have been observed which show significant stress amplitude changes occurring in times of 10^{-8} sec. It is the purpose of this paper to describe a new type of gauge capable of measuring either particle-velocity or stress with time-resolution limited only by the rise-time of the recording equipment and the planarity of the shock-wave front. The signal from the gauge results from the capacitance change of a solid dielectric disc which produces a current which is instantaneously proportional to the velocity of the stressed electrode.

We will first show an analysis which demonstrates the physical basis for the relationship between the shock-wave induced capacitance change and the current. Following this analysis, we will describe the experimental program used to study the properties of several promising materials and discuss the results obtained. This investigation shows that synthetic single crystal sapphire discs cut in the 60° orientation preferred growth habit are useful as gauges to stresses as high as about 100 kbar. These gauges have been used for the measurement of a number of stress-time profiles.

II. ANALYSIS OF A SHOCK-LOADED DIELECTRIC DISC

While a shock-wave is traversing a dielectric disc to which an electrostatic potential is applied, a current flows due to the shock-wave induced compression and permittivity change. To understand the behavior of a solid dielectric gauge, we must consider its response for time intervals which are short compared to the shock wave transit time. The analysis considers the response of the disc to a stress-time profile of arbitrary shape. The appendix includes an analysis of the response of the disc to a step function stress wave.

Consider a dielectric disc with an electrostatic potential between the electrodes on the two plane surfaces of the disc while one face of the disc is subjected to a rapidly changing impulsive load. Assume: (a) that the disc is in a state of one-dimensional strain, (b) that the electric field, E, in the disc is one-dimensional, (c) that the electrostatic potential difference, V, between the electrodes is constant, (d) that the electric field has the same value in the stressed and unstressed regions of the disc,[10] (e) that the stress is applied simultaneously to the entire electroded area, A, of the disc, and (f) that the current, i, resulting from the capacitance change flows in an external resistive load with a value such that the product of this resistive load and the capacitance of the gauge gives a time constant which is short compared to the risetime of the stress pulse.

Concerning the physical properties of the disc under shock-wave compression, assume: (g) that the resistivity is infinite, (h) that all stress amplitudes travel with the same velocity, U, (i) that all stress amplitudes are steady, (j) that the wave velocity is steady, (k) that the change in permittivity, ϵ, with particle velocity, u, is a constant which we will call ν, and finally (ℓ) that the disc exhibits no charge generation under shock.

For one-dimensional conditions, the displacement current, i(t), is written as

$$i(t) = A\, dD/dt \quad , \tag{1}$$

where t is the time and the electric displacement $D = \epsilon E$, may be evaluated as

$$\int_{x_o(t)}^{x_\ell} D(x)dx = \int_{x_o(t)}^{x_\ell} E\ \epsilon(x)dx \quad . \tag{2}$$

The x-direction is taken along the axis of the disc whose thickness is ℓ, and the position of the stressed electrode at $x = 0$ is taken to be time dependent. For a constant potential across the disc, Eq. (2) reduces to

$$D = \frac{V}{[\ell - x_o(t)]^2} \int_{x_o(t)}^{x_\ell} \epsilon(x)dx \quad . \tag{3}$$

The displacement current can then be evaluated from Eq. (1) and Eq. (3) as

$$i(t) = \frac{VA}{[\ell - x_o(t)]^2} \left\{ -\epsilon_o(t) \frac{dx_o}{dt} + \int_{x_o(t)}^{x_\ell} \frac{\partial \epsilon(x)}{\partial x} \frac{dx}{dt} dx + \frac{2 \frac{dx_o}{dt}}{[\ell - x_o(t)]} \left[\epsilon_i\big(\ell - x_o(t)\big) + \int_{x_o(t)}^{x=Ut} \gamma u(x)\ dx \right] \right\} \quad , \tag{4}$$

where dx_o/dt is the particle velocity $u(t)$ of the stressed electrode, $\epsilon_o(t) = \epsilon_i + \gamma u$ is the stressed permittivity and ϵ_i is the unstressed permittivity. Noting that the assumed steady properties of the wave give the condition that $dx/dt = -U$, Eq. (4) can be simplified to

$$i(t) = \frac{VAU}{\ell^2 [1 - \frac{x_o(t)}{\ell}]^2} \left[\gamma u(t) \left(1 - \frac{u(t)}{U} + \frac{2}{U[\ell - x_o(t)]} \int_{x_o(t)}^{Ut} u(x)dx \right) + \epsilon_i \frac{u(t)}{U} \right] \quad , \qquad 0<t<\ell/U \quad . \tag{5}$$

Three terms in Eq. (5), $[1 - \frac{x_o(t)}{\ell}]^2$, $\frac{u(t)}{U}$ and $\int u(x)dx$ depend upon the specific wave shape being considered and cause a time dependent response. However, it can be readily verified by reference to Eq. 5 that these contributions are of a magnitude (u^2/U) which is very small for small values of particle velocity. Neglecting these terms Eq. (5) simplifies to the expression

$$i(t) = \frac{VAU}{\ell^2} \left[\gamma u(t) + \epsilon_i \frac{u(t)}{U} \right] \quad , \qquad 0<t<\ell/U \quad . \tag{6}$$

Eq. 6 provides a relation between the instantaneous current and the instantaneous velocity of the stressed electrode. The first term in brackets gives the contribution due to the permittivity change and the second term gives the contribution due to the shock compression.

The analysis shows that for the highly restrictive assumptions used in the analysis and for small values of particle velocities the current is instantaneously proportional to the velocity of the input electrode for times before the rear electrode is stressed. The instantaneous nature of this response is analogous to that observed in the Sandia quartz gauge; however, the assumptions concerning the properties of the dielectric material must be verified experimentally. As we will demonstrate, Eq. (6) describes the observed response of sapphire with good precision for measurements as high as about 100 kbar.

III. EXPERIMENTAL INVESTIGATION

The instantaneous relation between the particle velocity of the input electrode and the current is obtained only under the restrictive conditions given in the analysis; hence, it is expected that only a very few dielectrics will actually respond as predicted in Eq. (6). In particular, assumptions (h), (i), and (j) require mechanical response which can only be obtained under elastic conditions. Since a high pressure gauge is of particular interest, potentially useful dielectric materials should have unusually large Hugoniot elastic limits. Accordingly, our attention is first directed toward such materials. After consideration of the elastic limits observed in several promising dielectrics, we will then describe measurements of dielectric properties under shock-wave compression.

Hugoniot Elastic Limit Measurements

Previous studies of single crystal quartz under shock-wave compression[11,12,13] show unusually high Hugoniot elastic limits even though the values observed depended upon the thicknesses of the samples and the driving pressure. X-cut samples have Hugoniot elastic limits of about 50 kbar while Z-cut samples exhibit a value of about 120 kbar. Since a Z-cut quartz disk is nonpiezoelectric, it is potentially useful as a solid dielectric gauge to stresses of about 120 kbar.

Sapphire, single crystal Al_2O_3, is noted for an extremely high elastic stiffness and a correspondingly high static tensile strength of 100 kbar in whisker form.[14] In addition, sapphire is now grown synthetically in sizes suitable for shock-wave experiments. Therefore, a determination of the Hugoniot elastic limit of sapphire is of immediate interest.

Measurements of the Hugoniot elastic limits of sapphire have been accomplished for three crystallographic directions;[15] the z-direction, the x-direction, and the easy synthetic growth direction which is nominally 60° from the z-direction.[16] It is beyond the scope of this paper to give a detailed account of these measurements, and they will be reported in more detail later. Briefly stated, however, the free surface velocity measurements (accomplished with a wire-reflection technique similar to that employed by Wackerle[11]) show that the Hugoniot elastic limit depends upon the driving pressure in a particular crystallographic direction. The lowest value obtained is 120 kbar for all three orientations at the lowest driving pressure of 200 kbar. Thus sapphire has the elastic properties required of a gauge for measurements of pressures to about 120 kbar. Because of the exceptionally high Hugoniot elastic limits of both quartz and sapphire, their dielectric properties can be observed under large elastic compressions.

Dielectric Measurements

Permittivities of solids under large compressions have not been extensively investigated even under static conditions. The permittivity of strontium titanate has been measured for pressures up to 50 kbar[17] while the permittivities of rubidium chloride, sodium chloride, and barium titanate have been measured for pressures up to about 25 kbar.[18,19,20] A number of other materials have been investigated at much lower pressures.[21,22] Previous shock-wave measurements of permittivity[2,23] are very limited and new experiments are needed with a more sensitive, generally applicable technique.

To induce shock-waves with precisely known amplitudes and well-defined profiles into our dielectric samples, we utilize controlled projectile impact experiments. The mechanical features of the experiment are the same as those previously reported for the investigation of the physical properties of X-cut quartz.[2] As indicated in Fig. 1, one dielectric disc, the specimen, is mounted on the muzzle end of a compressed gas gun. A second disc, the facing, of the same material is attached to the impact face of a projectile which is accelerated to various preselected velocities by the compressed gas gun.[24] The impact occurs in the evacuated barrel while the projectile is still guided by the bore of the gun barrel. Rigid control of all tolerances allows the impacting surfaces to be aligned to within 5×10^{-4} radian. This value for the "tilt" satisfies the required condition of achieving closure between the impacting surfaces in times short compared to shock-wave transit time across the specimen which is typically 250 nsec.

For symmetric impact, that is, the impact of identical materials, the particle velocity imparted to the specimen is exactly one-half the velocity of the impacting surface. This condition results for any material independent of the mechanical properties involved. If there is no stress relaxation,[25] the particle velocity is a constant until wave reflections occur. The impact velocity is measured to a precision of from 0.2% to 0.5% depending on the experiment;[26] thus, the particle velocity imparted to the sample is precisely specified and can be easily varied over a wide range.

For experiments within the elastic range, a single shock-wave propagates through the sample. For this condition the stress imparted to the sample can be computed from the conservation of momentum relation for a single stress jump into a medium at rest,

$$\sigma = \rho U u \quad , \qquad (7)$$

where σ is the x component of stress imparted to the sample and ρ is the undisturbed density. The particle velocity is determined from the impact velocity measurement while the shock-wave velocity is directly determined from the shock-wave transit time indicated on the electrical signal from the sample.

Similarly, from the conservation of mass relation the specific volume can be evaluated as

$$v/v_o = 1-u/U \quad , \qquad (8)$$

where v_o is the unstressed specific volume and v is the stressed specific volume.

Three dielectric materials in several crystallographic orientation have been investigated: Z-cut quartz, Z-cut and 60° sapphire,[15] X-cut and Z-cut ruby (Al_2O_3 + .05% Cr. doping). The axial alignment of the discs was within the specified crystallographic orientation to within 1 degree. The quartz was synthetic material hydrothermally grown by Sawyer Research Products. The sapphire and ruby were also synthetically grown by the Linde Co. using a flame fusion Verneuil process. All crystals were purchased from the Valpey Corp. who selected the material to flaw-free specifications, and subsequently shaped, polished and oriented the discs to ±1°. The plane surfaces of the discs were flat to 3 sodium light bands and the faces were parallel to 2.5×10^{-3} mm.[27] Typical disc dimensions were 19 to 25 mm in diameter and 1.5 to 2.5 mm in thickness. A state of one-dimensional strain is assured by using discs with diameter-to-thickness ratios of greater than 10.

Instrumentation

The seemingly contradictory electrical conditions require that the dielectric disc be biased with a constant electrostatic potential and that the pulsed signal from the disc be shunted with a resistive load. The circuit used consists simply of a charged coaxial cable[28] (unterminated) connected across the electrodes of the disc. The coaxial cable has the property that there is negligible D.C. potential difference between the power supply and the disc; but during shock-wave transit time, it acts as a 50 Ω resistive load. This load and the capacitance of the disc result in an R.C. time constant of about 10^{-9} sec which is short compared to the rise-time of the observed stress pulses. To obtain current pulses of the order of milliamps, electrostatic potentials of the order of kilovolts must be applied to the disc and detection circuit. The requirement for constant electrostatic potential is met since the observed transient signal is only one part in 10^4 of the static potential. Hence, the circuitry must also accommodate the additional static high voltage conditions. With the coaxial cable system the gauge can be biased, its current output loaded, and the current conducted to a location where it can be measured.

The coaxial cable used was 7/8-inch diameter air-dielectric[29] with a length of 95 meters beyond the coaxial probe connector to the oscilloscope. This system introduces negligible distortion between the voltage pulse measured at the oscilloscope and the current pulse output from the dielectric disc. The signal reflected from the open end of the cable does not interfere with the signal at the oscilloscope since the pulse duration is typically 250 nsec and the reflected pulse arrives 814 nsec later.

The connection to the oscilloscope is made with a low-loss coaxial capactive probe which blocks the electrostatic signal, yet admits the pulsed signal to the oscilloscope input. The oscilloscope used to display the transient signal was a high input impedance 85 MHz device[30] with a risetime of about 4 nsec. The oscilloscope traces were recorded photographically on high speed Polaroid film. The connection from the coaxial cable to the electrode is made with a short length of cable such that the inductance is less than 5 nhenry.

A low-noise regulated power supply[31] with accuracy of ±0.25% and less than 5 mv noise is used to apply the electrostatic potential across the disc through the cable as shown in Fig. 1. Typical signal levels are from 1 to 10 milliamp with typical bias voltages of from 500 to 2000 volts.

The sample assembly consists of an electrode disc of mild steel in intimate contact with the rear of the dielectric disc. The electrode is connected directly to the center conductor of the coaxial cable and this entire assembly is encapsulated in a low shrinkage epoxy resin inside a specimen holder. The coaxial cable ground shield connection is made between the input electrode and the ground ring by vacuum vapor deposited aluminum film across the impact face of the assembly. This film has a resistance of 0.1 ohm per square.

Results

A typical record obtained on 60° orientation sapphire at the relatively low stress amplitude of 30 kbar is shown in Fig. 2. The waveform corresponds very closely to the response predicted by Eq. (6). The finite risetime is a result of the closure time to impact the entire face of the disc. To confirm that the observed signals result from the capacitance change, experiments were conducted in which no electrostatic potential was applied to a sapphire disc shocked at 100 kbar. No signal was detected. Further, when voltage is applied to the disc the signals were found to scale according to the thickness, area, voltage, and wave velocity in the manner specified by Eq. (6). These considerations provide a direct verification that the observed currents result from the anticipated capacitance change of the dielectric discs under shock-wave loading.

The records obtained in the Z-cut quartz experiments showed considerable "noise" at all stress levels. Further, the signals showed distortions resulting from excessive internal conduction at all stress levels. Thus, even though current amplitudes showed a linear increase with stress from 25 to 70 kbar Z-cut quartz is not suitable for a gauge material.

As both the strain and permittivity change become large at the higher stress amplitudes, the factors neglected in deriving Eq. (6) become detectable and the current profile deviates from a constant value. The solution given in the appendix for the current resulting from a constant amplitude shock-wave shows that for the values of capacitance change observed at 100 kbar for the 60° orientation the current should decrease 12% during wave transit time. To provide for this effect the current value used to characterize the data is the jump in current, i_i, observed at impact time. As indicated by Eq. (6), it is possible to separate the experimentally adjustable parameters ℓ, A, and V from the physical properties U, ϵ, and γ. Thus, a factor $I \equiv i_i \ell^2/AV$, called the scaled capacitive current, specifies the current jump obtained at a given particle velocity. The values observed for γ were negative for all the material investigated. That is to say, the permittivity decreased with increasing stress.

The scaled capacitive current values observed for two crystallographic orientations of ruby are shown in Fig. 3. These values for both the x and z direction show a pronounced change in slope at particle velocities between 0.09 and 0.11 mm/μsec (40 to 50 kbar). This arises from a nonlinear permittivity change and prevents use of ruby as a time-resolved gauge for stress above about 40 kbar. Further, both ruby orientations show excessive internal conduction for stress amplitude above 50 kbar. Thus ruby discs can be employed as time-resolving stress gauges to stresses up to only 40 kbar.

The values obtained for the two sapphire orientations are shown in Fig. 4. Both orientations show linearly increasing values of I with increasing stress. Again, however, for stresses greater than about 40 kbar the Z-cut discs show excessive internal conduction, and a time-resolving gauge in this orientation will be limited to measurements below 40 kbar.

The response of the 60° orientation sapphire discs is more encouraging in that I increases linearily with particle velocity and the resistivity under shock remains much higher than for the other materials investigated. Up to a stress of about 75 kbar the resistivity remains high enough such that it has no effect on the records. Above 75 kbar internal conduction becomes detectable and at 100 kbar causes the current to decrease about 25% during wave transit time. At this same stress a 12% decrease is predicted for the step function stress input (see appendix). This effect is not expected to affect stress readings of sharply rising wave fronts but would appreciably affect wave profiles with slowly rising stress amplitudes. Thus, 60° sapphire has the dielectric properties required for a solid capacitance gauge in a useful pressure range, and we will consider the mechanical properties of this material in more detail.

Mechanical Property Measurements

The quality of synthetic sapphire grown in the 60° orientation is generally much better, and the material is more readily available than other orientations because this is the preferred growth direction. However, from the standpoint of its elastic properties this orientation would not have been an obvious choice for a gauge material. The elastic response is somewhat uncertain since this orientation is not a "specific"[32] direction. Generally, an anisotropic crystal responds to a longitudinal motion with both shear and longitudinal components except in "specific" directions which give pure longitudinal motion. Since the 60° orientation is not a specific direction, it is possible that a shear wave might be produced and propagate through the crystal at a velocity much slower than the longitudinal velocity. The current-time measurements are very sensitive to the properties of the shock-wave. If a slower moving stress wave of significant amplitude were present in the disc, it would be expected to affect the amplitude and time dependence of the current. There is no evidence for the presence of a slower moving wave in any of the records.

In order to explore the mechanical response of 60° discs in more detail, an additional experiment was performed. A specimen disc 12.7 mm thick was impacted at 30 kbar with a quartz gauge to measure the stress and particle velocity imparted to the disc. An additional quartz gauge located at the rear of the sapphire specimen recorded the arrival of the stress pulse produced by the impact. This "front-back" experiment[33,34] permits two independent evaluations of the mechanical properties of the impacted specimen on the same experiment. A delayed arrival of a shear wave would be easily detected. The experiment showed a single longitudinal shock-wave arriving at the rear quartz gauge. The amplitude of this wave agreed within experimental error with the stress value measured at the impact surface. The propagation velocity of the wave also agreed with that determined from the capacitance change measurements. Thus, it appears that a single longitudinal shock-wave propagates within the elastic range of 60° orientation sapphire. Even though this orientation is not a specific direction, sapphire shows a very symmetrical elastic response in the various directions.[35,36] (For example, the elastic constant c_{11} is numerically equal to the elastic constant c_{33}.) For that reason one might expect that the anistropic response is too small to be detectable.

The appreciable deformation encountered in the elastic range of sapphire (about 2% at 100 kbar) would be expected to cause some small increase in wave velocity over the low signal value. The transit time measured from our capacitance change records give a direct measurement of the wave velocity. In addition, wave velocity measurements were obtained on the previously described quartz gauge experiment and the free-surface-velocity measurements[15] to determine the Hugoniot elastic limit. The precision of the wave velocity measurements made from the capacitance change records is presently limited to ±1%. The precision of the other two experiments is ±1/2%. The linear fit to these data is $U = 10.96 + 0.98\ u$, where U and u are given in mm/μsec. This fit shows the wave velocity to increase 2% at 100 kbar. This small change in wave velocity with increasing particle velocity will have only a minor influence on gauge performance.

IV. SUMMARY AND CONCLUSIONS

This paper has shown the analytical basis for the use of the capacitance change of a solid dielectric disc for time-resolved stress or particle velocity measurements. An experimental method for studying the permittivity change induced by the one-dimensional strain shock-wave loading was developed and applied to the study of quartz, ruby, and sapphire discs. Sapphire in the 60° orientation is found to have appropriate properties for use as a gauge for stress pulses of arbitrary shape to 75 kbar and for the measurements of stress jumps to 100 kbar. Ruby and sapphire in the z and x directions could be used as gauges up to stresses of about 40 kbar. A more detailed study of the 60° orientation discs is required to obtain more data in smaller stress increments and to investigate the higher stress region in more detail.

The major limitation for use of the sapphire gauge is the short recording time (typically 250 nsec) limited by the wave transit time in the gauge. This is sufficient time for meaningful observations on jumps in stress but multiple wave fronts such as are encountered in elastic-plastic wave propagation studies generally require more observation time. However, measurements on thin samples are easily accomplished as indicated by the record shown in Fig. 5. This sapphire gauge record shows a measurement of the elastic-plastic wave profile propagated through a sample of spheroidized 4340 steel. The elastic wave amplitude is 21 kbar, and the plastic wave amplitude is 75 kbar. Other measurements recently accomplished with the sapphire gauge include a Hugoniot elastic limit determination on [100] germanium (53 kbar) and a determination of a first-order phase transition in a 20 Cr 8.5 Ni stainless steel at 70 kbar.

The gauge seems immediately applicable to impact surface measurements of mechanical properties as previously described.[32] One very desirable feature of the sapphire gauge is that it has a high acoustic impedance (very close to that of steel) and as such allows direct measurements of wave profiles in high impedance materials without wave reflections. In practice we find the sapphire gauge no more difficult to use than the quartz gauge. The sapphire gauge unit is easier to assemble than the quartz gauge because a guard-ring configuration is not used, and it does not seem necessary in the configurations tested.

The milliampere signal level is somewhat restrictive compared to the ampere signal level achieved with the quartz gauge. However, we are currently using gauges 38 mm in diameter and 2.5 mm thick which give a current of 4 ma at 23 kbar when an electrostatic potential of 2 kilovolts is applied. This signal level is high enough for reasonably easy measurements.

It should be emphasized that the general concept used for the solid capacitance gauge is potentially applicable to materials other than sapphire. Although it is doubtful that many materials will be useful to 100 kbar, it is certainly conceivable that a number of materials may be useful at lower stress levels. It may be advantageous to use other materials at low stresses in order to do impedance-matched experiments. The analysis and experiments reported in this paper show the conditions for which these solid capacitance gauges will operate.

Appendix

Capacitance Change From A Constant Amplitude Stress Pulse[37]

The analysis given for current produced by the capacitance change resulting from a stress pulse of arbitrary shape neglects the effect of the slightly different electric field in the stressed and unstressed regions of the disc. The effect of neglecting this can be evaluated by deriving the current expected from a constant amplitude stress wave. The analysis makes use of the same assumptions as in the main text except that no restriction is placed on the value of the electric fields in the various regions of the discs. In what follows, the subscript (1) refers to the unstressed region, and the subscript (2) refers to the stressed region.

Since the electric displacements are equal in the stressed and unstressed region of the disc

$$\epsilon_1 E_1 = \epsilon_2 E_2 \quad . \qquad \text{A-1}$$

The constant electrostatic potential between the electrodes require that

$$E_2(U-u)t + E_1(\ell-Ut) = V \quad . \qquad \text{A-2}$$

Solving for E_1 from Eq. A-2 and substituting this value into A-1 gives

$$E_2 = \frac{\epsilon_1 V}{\epsilon_1(U-u)t + \epsilon_2(\ell-Ut)} \qquad \text{A-3}$$

Solving for the displacement current and collecting the various terms yields

$$\frac{i\ell^2}{AV} = \frac{\gamma u[1+u/U] + \epsilon[u/U+(\gamma u/\epsilon)^2]}{[(1-ut/\ell) + \frac{\gamma u}{\epsilon}(1-Ut/\ell)]^2} \quad , \qquad \text{A-4}$$

where ϵ is the unstressed permittivity.

This result shows that the effect of the constant field assumption is principally to neglect terms in $(\gamma u/\epsilon)^2$ which are second order terms in the change in permittivity. The largest effect will be at the highest stress encountered. Comparing the solution of Eq. A-4 to Eq. 6 for the values obtained for 60° sapphire at 100 kbar we find that Eq. A-4 gives a current 8.5% higher than Eq. 6 at $t = 0$ and a current 4.0% lower at $t = \ell/U$. Thus, the true response shows a decrease in current of 12.4% at 100 kbar. This effect will not cause serious difficulties in the gauge response.

Acknowledgement

The authors are pleased to acknowledge the Hugoniot elastic limit measurements performed by W. P. Brooks, helpful discussions with E. B. Royce, and many Sandia Corporation colleagues.

References and Footnotes

1. O. E. Jones, F. W. Neilson, and W. B. Benedick, J. Appl. Phys. 33, 3224 (1962).

2. R. A. Graham, F. W. Neilson, and W. B. Benedick, J. Appl. Phys. 36, 1775 (1965).

3. M. H. Rice, Rev. Sci. Instr. 32, 449 (1961).

4. John W. Taylor and Melvin H. Rice, J. Appl. Phys. 34, 364 (1963).

5. A. G. Ivanov, S. A. Novikov, and V. A. Sinitsyn, Fizika Tverdogo Tela 5, 269 (1963).

6. A. G. Ivanov, S. A. Novikov, Pribory i Tekhnika Eksperimenta 1, 128 (1963).

7. L. M. Barker and R. E. Hollenbach, Rev. Sci. Instr. 36, 1617 (1965).

8. L. M. Barker, B. M. Butcher, and C. H. Karnes, J. Appl. Phys. 37, 1989 (1966).

9. L. M. Barker, Proceedings this Conference.

10. This assumption is basically in error since the permittivities of the stressed and unstressed regions of the disc are different. However, the effect of neglecting this is small. The extent of the effect can be evaluated from the analysis given in the appendix.

11. Jerry Wackerle, J. Appl. Phys. 33, 922 (1962).

12. G. R. Fowles, Stanford Research Institute, Poulter Laboratories Technical Report 003-61 (1961).

13. G. A. Adadurov, A. N. Dremin, S. V. Pershin, V. N. Rodionov, and Yu. N. Ryabinin, Zhurnal Prikladnoy Mekhaniki i Tekhnicheskoy Fiziki 4, 81 (1962).

14. S. S. Brenner, J. Appl. Phys. 33, 33 (1962).

15. W. P. Brooks and R. A. Graham, Bull. Am. Phys. Soc. 11, 414 (1966).

16. This direction is actually 57° from the z-direction; however, we will use the normal terminology applied to this orientation and call it the 60° orientation.

17. G. A. Samara and A. A. Giardini, Phys. Rev. 140, A954 (1965).

18. G. A. Samara, Solid State Communications 4, 279 (1966).

19. J. A. Corll and G. A. Samara, Solid State Communications 4, 283 (1966).

20. G. A. Samara, Phys. Rev. 151, 378 (1966).

21. D. F. Gibbs and M. Jarman, Phil. Mag. 7, 663 (1962).

22. D. F. Gibbs and G. J. Hill, Phil. Mag. 9, 367 (1964).

23. G. E. Hauver, J. Appl. Phys. 36, 2113 (1965).

24. S. Thunborg, G. E. Ingram, and R. A. Graham, Rev. Sci. Instr. 35, 11 (1964).

25. Experiments can be conducted at stresses well below the elastic limit where stress relaxation would not be expected to occur and then increased to higher stress levels. The electrical signal from the sample (to be described later) permits further definition of the mechanical behavior because the signal depends upon both electrical and mechanical properties of the disc. Mechanical relaxation effects would produce a noticeable progressive deterioration in the electrical response with increasing input stress.

26. G. E. Ingram, Rev. Sci. Instr. 36, 458 (1965).

27. The tolerances of some of the discs used in the early experiments did not meet such precise specifications.

28. For a more detailed description of the properties of charged coaxial cables see I.A.D. Lewis and F. H. Wells, Millimicrosecond Pulse Techniques, Pergamon Press, New York, (1959).

29. "Heliax cable" manufactured by the Andrew Corporation.

30. Tektronix Model RM585A Type 86 preamplifier.

31. Fluke Model 410B High Voltage Regulated Power Supply.

32. R. F. S. Hearmon, An Introduction to Applied Anisotropic Elasticity, Oxford University Press (1961).

33. W. J. Halpin, O. E. Jones, and R. A. Graham, in "Symposium on Dynamic Behavior of Materials," ASTM Special Technical Publication No. 336, American Society for Testing and Materials (1963).

34. W. J. Halpin and R. A. Graham, Proceedings Fourth Symposium on Detonation U. S. Naval Ordnance Laboratory (1965).

35. J. B. Wachtman, W. E. Teft, D. G. Lam, Jr., and R. P. Stinchfield, Journal of Research, National Bureau of Standards 64A, 213 (1960).

36. B. T. Bernstein, J. Appl. Phys. 34, 169 (1963).

37. The result obtained in this analysis is similar to one obtained by E. B. Royce, Lawrence Radiation Lab., University of California.

Figure Captions

Fig. 1. Schematic diagram showing the shock loading method and the charged coaxial cable instrumentation system.

Fig. 2. Typical current pulse resulting from a 60° orientation sapphire disc impacted symmetrically at 30 kbar. Time increases from left to right. The wave transit-time is about 250 nsec. The timing wave shown above the gauge signal is 50 MHz while the lower trace is a voltage calibration.

Fig. 3. Scaled capacitive current values observed for the ruby discs. With wave velocities of 11.1 mm/μsec and a density of 3.986 g/cm3, a particle velocity of 0.1 mm/μsec is associated with a stress of 44.2 kbar. The wave velocity changes only about 2% in the particle velocity range shown.

Fig. 4. Scaled capacitive current values observed for the sapphire discs. With wave velocities of 11.1 mm/μsec and a density of 3.986 g/cm3, a particle velocity of 0.1 mm/μsec is associated with a stress of 44.2 kbar.

Fig. 5. Stress-time profile observed with a sapphire gauge on a sample of spheroidized 4340 steel which is 3.18 mm thick. Time increases from left to right. The gauge recording-time is about 250 nsec. The maximum stress observed is 75 kbar. A timing fiducial is shown before the arrival of the elastic wave. The propagation of the elastic wave through the rear electrode of the gauge causes the inverted signal observed late in the trace. The small amplitude sinusoidal trace at the bottom of the figure is a 50 MHz timing wave and the larger amplitude trace is the voltage calibration.

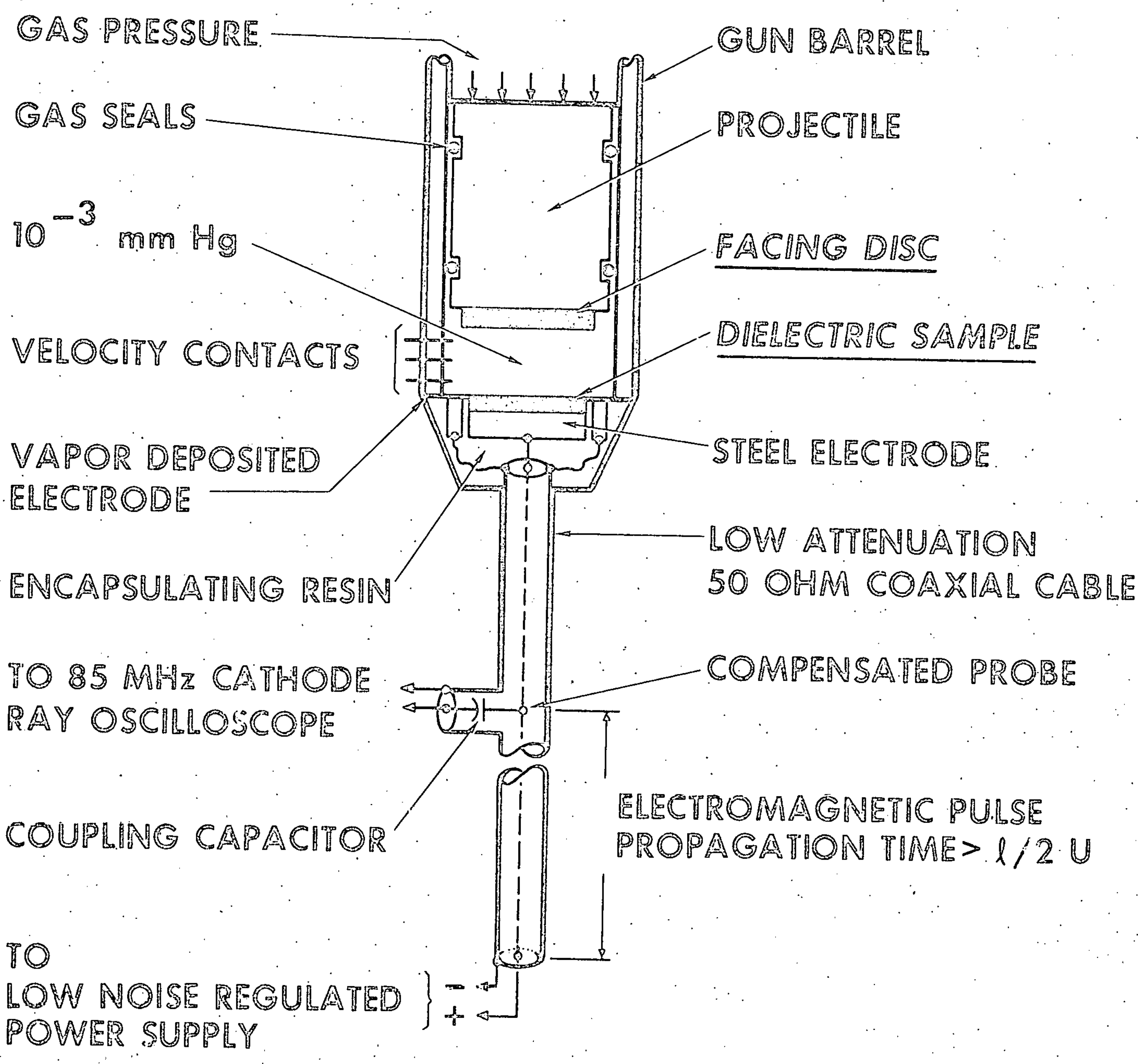
GAS PRESSURE
GUN BARREL
GAS SEALS
PROJECTILE
10 -3 mm Hg
FACING DISC
VELOCITY CONTACTS
DIELECTRIC SAMPLE
VAPOR DEPOSITED ELECTRODE
STEEL ELECTRODE
ENCAPSULATING RESIN
LOW ATTENUATION 50 OHM COAXIAL CABLE
TO 85 MHz CATHODE RAY OSCILLOSCOPE
COMPENSATED PROBE
COUPLING CAPACITOR
ELECTROMAGNETIC PULSE PROPAGATION TIME> l/2 U
TO LOW NOISE REGULATED POWER SUPPLY
-
+

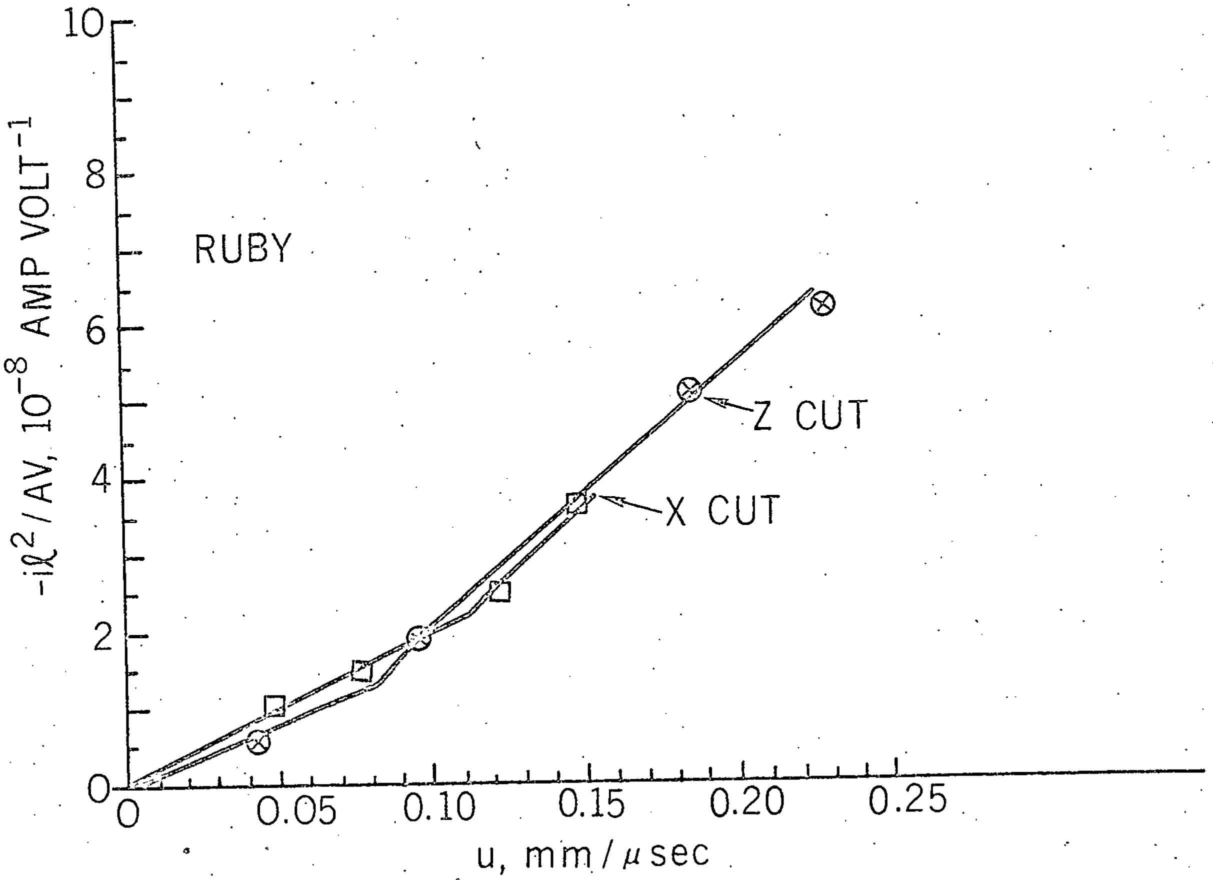
10
8
6
4
2
0
$-i\ell^2/AV$, 10^{-8} AMP VOLT^{-1}
RUBY
Z CUT
X CUT
0
0.05
0.10
0.15
0.20
0.25
u, mm/μsec

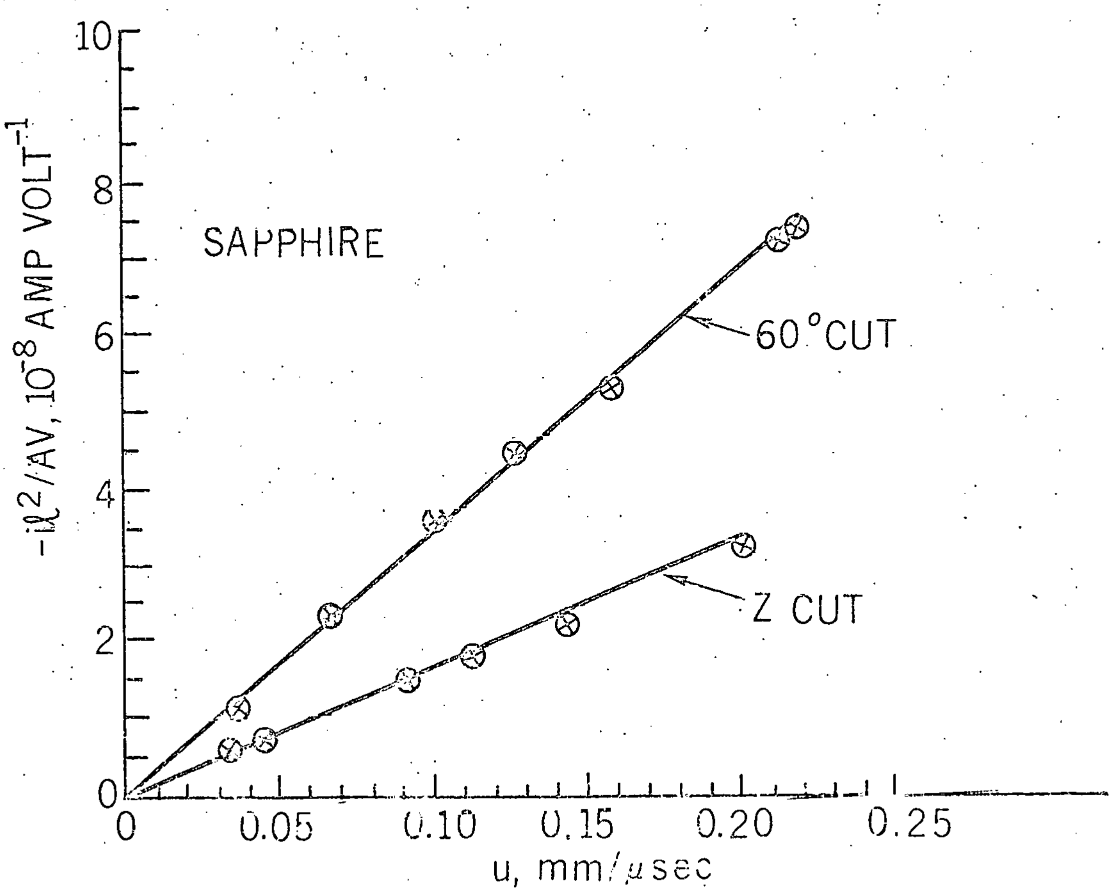
10
8
6
4
2
0
$-i\ell^2/AV$, 10^{-8} AMP VOLT^{-1}
SAPPHIRE
60°CUT
Z CUT
0
0.05
0.10
0.15
0.20
0.25
u, mm/μsec